JOURNAL OF APPLIED POLYMER SCIENCE VOL. 12, PP. 1119–1136 (1968)

Influence of Molecular Weight on Some Properties of Poly(vinyl Chloride)

GIOVANNI PEZZIN and GIUSEPPE ZINELLI, *Montecatini-Edison S.p.A. and Istituto di Chimica Fisica, Università di Padova, Italy*

Synopsis

Several fractions obtained from a large-scale fractionation and several unfractionated PVC polymers and blends have been processed both as rigid and plasticized compounds. The latter have been studied by stress–strain, creep, and recovery tests. The recoverable character of the creep results show that a relatively stable network must be present in the samples. The crosslink density is little influenced by molecular weight, as shown by the modulus and compliance results. On the contrary, the ultimate tensile properties depend strongly on molecular weight, which is interpreted as evidence that the stability of the crosslinks increases with increasing chain length of the polymers.

INTRODUCTION

Relatively little information is available on the effect of molecular weight and of molecular weight distribution (MWD) on the physical properties of poly(vinyl chloride). In order to investigate the influence of these variables on the mechanical and melt flow properties, a number of fractions varying in average molecular weight has been obtained from a large-scale fractionation. A series of unfractionated polymers of widely different molecular weights have also been prepared and then characterized by dilute solution techniques. The results of the study of some properties of these fractions and polymers and of mixtures thereof are described in the present paper.

In the preparation of samples for similar studies any mechanical or thermal degradation of the samples should be avoided. Since this is almost impossible for unplasticized PVC formulations, most of the work has been done on plasticized specimens, since their processing can be accomplished without appreciable degradation.

EXPERIMENTAL AND RESULTS

Materials

Eleven fractions, ranging in number-average molecular weight $\bar{M}_n$ from 2.5×10^4 to 10^5, have been obtained from a large-scale fractionation.[1] Eight polymers, having $\bar{M}_n$ from 4×10^3 to 10^5, have been polymerized in suspension between 35 and 70°C., by standard procedures. Small amounts

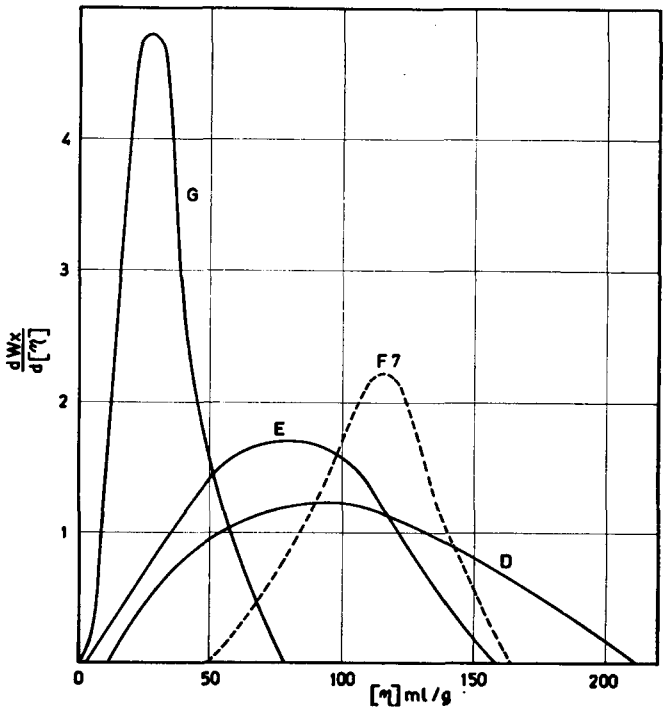

Fig. 1. Differential weight distribution curves of some polymers. The curve for fraction 7 is plotted for comparison.

of a crosslinking agent or large amounts of a chain-transfer agent (tetrahydrofuran), have been added to the polymerizing mixtures in order to obtain the highest and the lowest molecular weight samples, respectively. Six samples with large MWD have been prepared from fractions or polymers of different molecular weights by mixing dilute solutions of the components in the weight ratio 50/50.[2]

The molecular properties of the fractions are described elsewhere;[1] those of the polymers and blends are listed in Table I. The $\bar{M}_n$ and $\bar{M}_w$ of the integral polymers were measured directly by osmometry and light scattering. For the blends these values were calculated from those of the components.[2] Some molecular weight distribution curves, determined by fractional precipitation in the system tetrahydrofuran–water, are shown in Figure 1, where the curve for fraction 7 is plotted for comparison. Some skewness to the low molecular weight side is shown by samples D and G. It must be noted that the MWD of the fractions is not much narrower than that of the unfractionated polymers, the heterogeneity indices $\bar{M}_w/\bar{M}_n$ being, respectively, about 1.8 and 2.2. The blends have bimodal distribution curves and their calculated heterogeneity indices are larger. The glass transition temperatures T_g of the samples, measured by differential scanning calorimetry, are also listed in Table I. Those of the fractions have been reported previously.[1]

TABLE I
Characterization of PVC Polymers and Blends

Sample	Polymerization temperature, °C.	Composition	Chlorine content, %	Intrinsic viscosity, ml./g.	$\bar{M}_n \times 10^{-3}$	$\bar{M}_w \times 10^{-3}$	$\bar{M}_w/\bar{M}_n$	T_g, °C.
Polymers								
A	35		—	190	100	(200)	2.0	79
B	40		56.3	151	84	175	2.1	81
C	51		56.4	135	75	150	2.0	76
D	51		56.2	102	53	130	2.4	75
E	57		56.3	78	40	90	2.2	75
F	67		56.2	70.5	32	70	2.2	74
G	62		55.7	31	8.5	26	3.0	64
H	72		55.4	14.5	4.0	10	2.5	58
Blends								
B1		F3 + F10	55.8	107	55	120	2.2	75
B2		F4 + F11	55.7	98	40	114	2.9	73
B3		F7 + F9	55.5	97	64	116	1.8	73
B4		A + G	55.8	108	77	105	13.6	—
B5		A + H	56.0	108	16	113	7.0	—
B6		B + F	56.2	110	46	123	2.7	77

The T_g values range from 73°C. to 80°C. for all samples, except for polymers G and H for which $\bar{M}_n$ is below 10^4.

It is known that the properties of polymers are influenced not only by molecular weight and MWD, but also by such variables as chain branching, stereoregularity, and crystallinity.

However for the PVC samples here investigated these variables should not play a major role. The branching index has been found to be about 1.7 endgroups per hundred carbon atoms both for the fractions[1] and for the unfractionated polymers.[3]

The stereoregularity and crystallinity degrees should not differ appreciably for PVC samples polymerized between 35 and 70°C.[4-6] unless the molecular weight of the polymer is very low, in which case the crystallinity has been claimed to increase.[7] This effect should however be sensible only for polymer H, which has $\bar{M}_n$ = 4000 (see Table I). With this exception, it is safe to assume therefore that the physical properties investigated are dependent only on molecular weight and MWD.

Unplasticized Samples

Unplasticized specimens of all the fractions, of the blends B1, B2, and B3, and of polymers B to F (polymers G and H were not studied because of their brittleness) were obtained by roll milling at 190°C. for about 5 min. the PVC samples with 2% of a lead stabilizer, and molding the compounds at 190°C. into molds of dimensions suitable for physical testing (1 × 10 × 100 mm.).

The molecular weights of the molded specimens were followed after dissolution in cyclohexanone, centrifugation, precipitation in methanol and drying, by measuring the intrinsic viscosity of the recovered polymers. It was found that the compounding and molding caused marked shear and/or heat degradation, the values of $[\eta]$ being about 20% lower than that of the original samples. Since the formation of insoluble reticulated polymer is also possible in the processing of rigid PVC,[8] the molecular characteristics of the samples are probably severely modified with respect to those listed in Table I. For these reasons, only few physical properties of the unplasticized PVC samples have been measured. Stress–strain curves have been determined at 23°C. on the Instron tensile tester, following ASTM D638, at a crosshead speed of 0.5 cm./min., on specimens having an unstrained length of 5.0 cm. The results did not reveal significant effects of molecular weight or MWD. The Young's modulus at 1% elongation was found to be $2.6 \pm 0.4 \times 10^{10}$ dyne/cm.^{2}, and the elongation at break showed too large a variability within tests on individual PVC samples to give any indication of effects of molecular weight.

Similar results were found for the dynamic-mechanical properties, measured at about 1 cps by means of a free oscillation torsion pendulum. No substantial differences of the mechanical damping were found in the glassy region, and only the main transition of the low molecular weight samples was found to fall at lower temperatures.

Plasticized Samples

All the fractions[1] and the samples listed in Table II were investigated in the form of plasticized compositions. They were dry-blended with 60 parts of dibutyl phthalate, which is one of the most efficient plasticizers, and 2.2 parts of a lead stabilizer. The volume fractions of PVC and plasticizer are about 0.55 and 0.45, respectively.

TABLE II
Conditions and Results Plastograph Tests and Glass Transition Temperatures T_g of the Plasticized Polymers

Sample	Roller temperature, °C.	Melt temperature, °C.	Equilibrium torque T (arbitrary units)	T_g, °C.
F1	170	180	990	−31
F2	156	168	1200	
F3	156	167	1180	−34
F4	156	163	1050	
F5	152	160	900	
F6	156	158	800	
F7	156	158	740	
F8	156	158	670	−30
F9	151	151	540	
F10	151	151	245	−40
F11	151	151	120	−38
A	173	178	1090	−45
B	160	166	1030	
C	159	159	700	−38
D	155	155	680	
E	151	151	480	
F	151	151	300	−39
G	150	150	80	−48
H	150	150	—	−48
B1	157	157	460	−42
B2	157	157	410	
B3	157	157	560	
B4	166	166	290	−46
B5	151	151	340	
B6	151	151	550	

The plasticization was carried out between 150 and 180°C. in the Brabender Plastograph,[9] with the use of a 45-g. mixing head of the roller type (which approximates the action of a Banbury mixer) turning at 50 rpm. The temperature of the mixture was measured by means of a thermocouple immersed in the melt. The roller temperature, controlled by circulation of thermostatted silicon oil, was also recorded. The deformation power measured by the instrument usually reaches a plateau, after an initial peak, as shown in Figure 2 for the PVC fractions. The roller and polymer temperature and the equilibrium torque T are listed in Table II. It is seen that for high molecular weight samples the melt temperature is about 10°C. higher than the chamber temperature, due to the viscous heat pro-

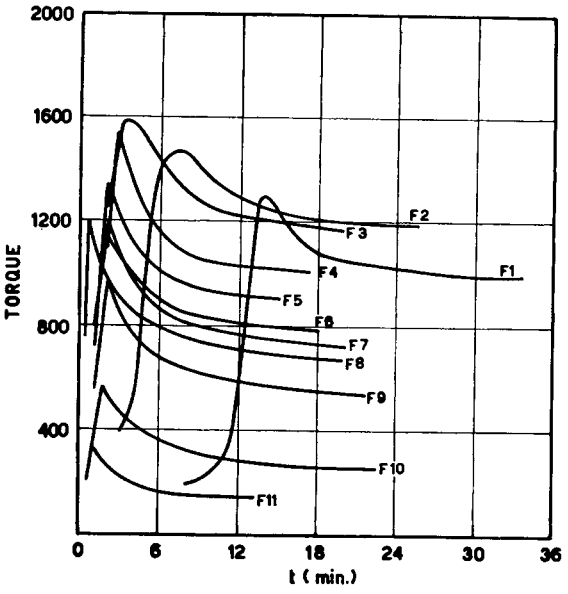

Fig. 2. Torque–time curves for the plasticized PVC fractions. The temperature conditions and the equilibrium torques for all samples are reported in Table II.

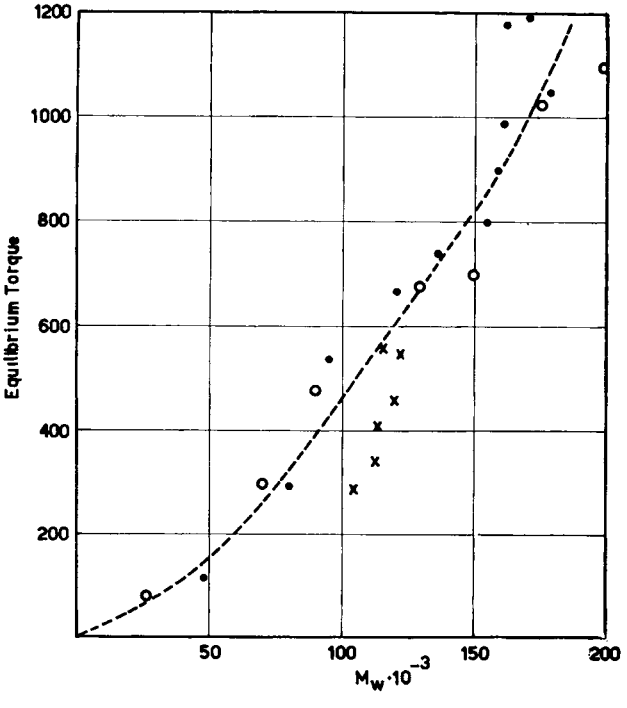

Fig. 3. Equilibrium torque plotted vs. weight-average molecular weight M_w: (●) fractions; (○) unfractionated polymers; (×) blends.

duced by the intense shearing. The torque–time curves show an initial peak due to the gelation process, i.e., to polymer–plasticizer interaction.[10] As is usual for good plasticizers, the gelation time is of the order of few minutes for all samples, except for fraction 1 and polymer A. The torque at the plateau measures the total resistance to deformation of the plasticized polymer at the temperature and shear conditions of the mixing head. A plot of the equilibrium torque versus $\bar{M}_w$ is shown in Figure 3 (for fractions 1 and 2 $\bar{M}_w$ values of 160,000 and 170,000 are used[1]).

A correlation between T and $\bar{M}_w$ exists only for fractions and polymers, while the blends have equilibrium torques lower than those of fractions and polymers of equivalent $\bar{M}_w$.

Specimens suitable for physical testing were obtained from the plasticized compounds taken from the plastograph at equilibrium by compression molding for 3 min. at 160 ± 5°C. and at pressures of the order of 50–70 kg./cm.^{2}. Their glass transition temperatures T_g are reported in Table II. The density of the samples, measured pycnometrically at 23°C., was found to be 1.279 ± 0.002 g./ml.

A check of the dilute solution viscosity of these samples after precipitation showed that no degradation of the PVC had taken place, so that the molecular data listed in Table I should still characterize the plasticized samples.

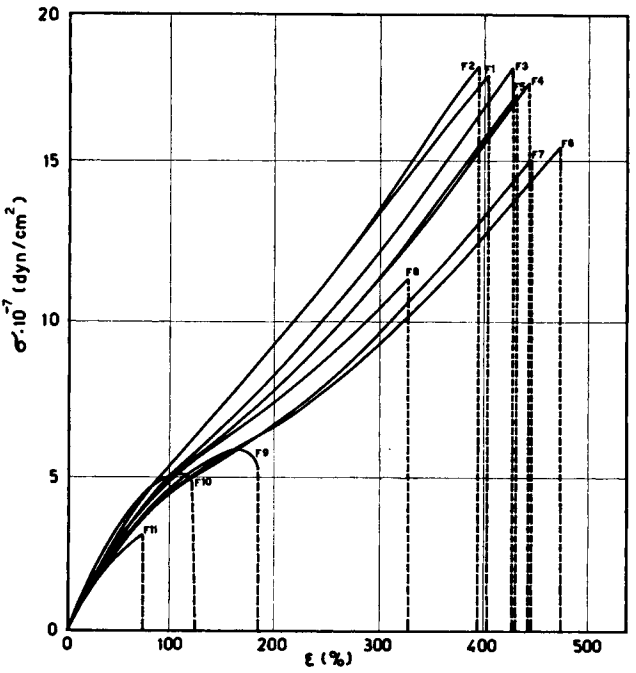

Fig. 4. Tensile stress σ vs. elongation • for the plasticized fractions at 23°C. and 4.2% strain/sec.

Stress–Strain Measurements

The stress–strain behavior of the plasticized samples was investigated at 23°C. by means of the Instron tensile tester, on square-end dumbbell-shaped specimens having a gage length of 20 mm. and a cross-section of 8 mm.^{2}. The crosshead speed was 5 mm./min., corresponding to a strain of 4.2%/sec. Typical curves of tensile stress σ versus strain ϵ are plotted in Figure 4. From the slope of the initial linear portion, which extends up to elongations of about 25%, the Young's modulus E has been calculated. The most important ultimate property is the tensile strength σ_B, which has been calculated as the tensile load at break divided by the original cross-sectional area. The energy to break A is given by eq. (1)

$$A = \int_0^{\epsilon_B} \sigma d\epsilon \tag{1}$$

where ϵ_B is the elongation at break; this was obtained by graphical integration of the stress–strain curves.

The results are collected in Table III, where each figure is the average value of the results of ten tensile tests. The reproducibility was generally

TABLE III
Tensile Properties of the Plasticized Samples at 23°C.

Sample	Young's modulus $E\times10^{-7}$, dyne/cm.^{2}	Tensile strength $\sigma_B\times10^{-7}$, dyne/cm.^{2}	Elongation at break ϵ_B, %	Energy to break $A\times10^{-7}$, erg/cm.^{2}
F1	7.2	17.7	400	78
F2	6.5	17.4	395	71
F3	6.2	17.4	420	77
F4	6.0	17.0	440	76
F5	6.2	16.6	435	72
F6	5.6	15.5	470	77
F7	6.0	15.2	440	70
F8	6.5	10.9	320	41
F9	6.0	5.7	180	14
F10	7.2	4.6	120	7.6
F11	6.2	3.0	74	2.5
A	7.4	19.1	420	86
B	7.7	19.3	435	83
C	8.1	13.3	315	48
D	6.9	12.7	395	52
E	6.7	8.2	290	28
F	5.2	4.9	210	12
G	3.6	1.6	60	1.0
H	1.1	0.37	45	0.34
B1	5.9	9.6	345	39
B2	6.4	11.1	415	49
B3	6.5	9.5	316	34
B4	6.0	9.6	480	54
B5	6.2	8.1	330	32
B6	5.3	11.8	395	48

of the order of a few per cent. The effect of molecular weight is shown in Figures 5–8, where the weight-average molecular weight $\bar{M}_w$ has been used.

Plots of the ultimate tensile properties versus the number-average molecular weight $\bar{M}_n$ are more scattered, and the data for blends do not correlate with those for the other samples. From Figure 5 it is seen that the Young's modulus E is largely independent of $\bar{M}_w$ above $\bar{M}_w = 4 \times 10^4$.

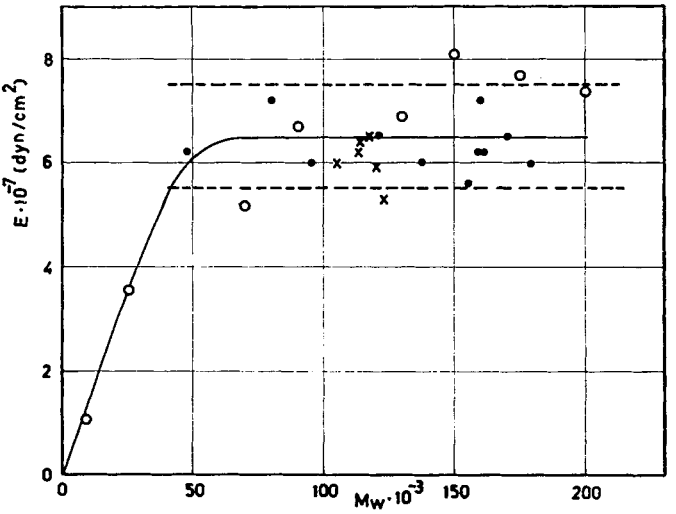

Fig. 5. Young's modulus E vs. M_w. Symbols same as in Fig. 3.

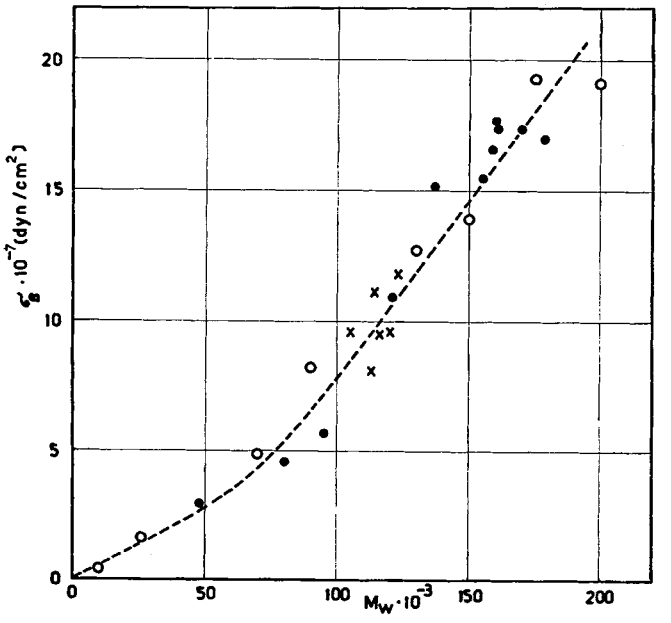

Fig. 6. Tensile strength σ_B vs. M_w. Symbols same as in Fig. 3.

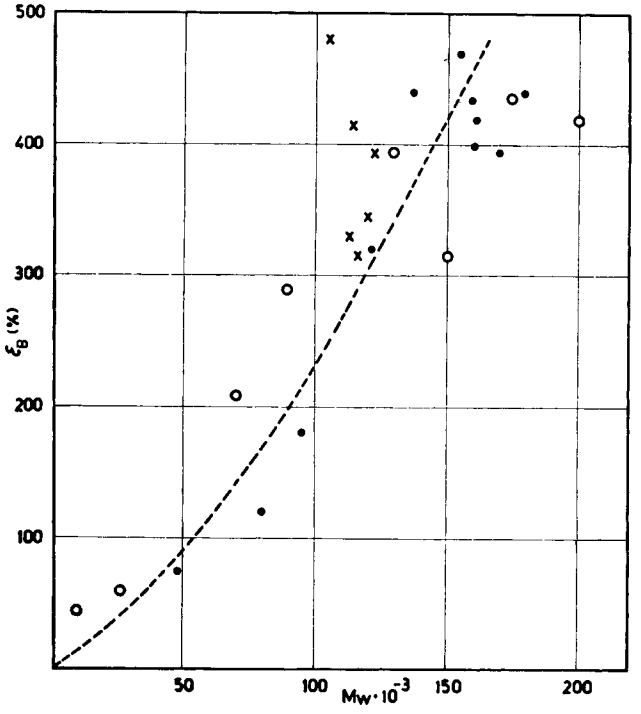

Fig. 7. Elongation at break ϵ_B vs. M_w. Symbols same as in Fig. 3.

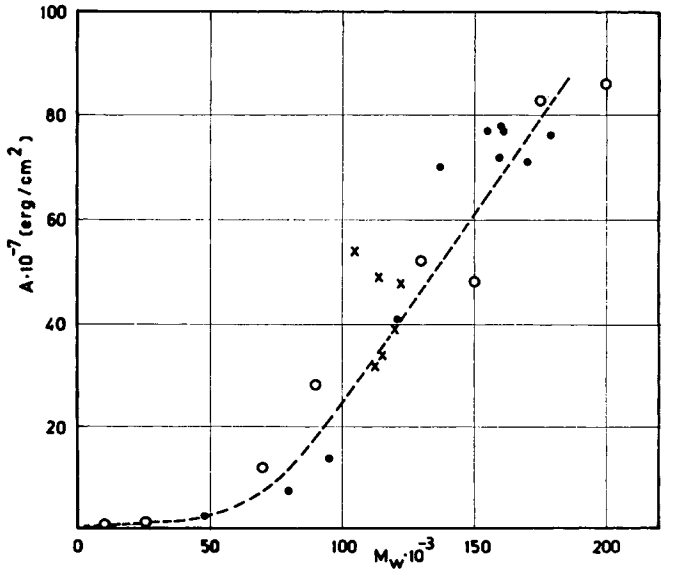

Fig. 8. Energy to break A vs. M_w. Symbols same as in Fig. 3.

On the contrary, the ultimate properties σ_B, ϵ_B, and A increase with increasing molecular weight without leveling off at large values of $\bar{M}_w$ (Figs. 6–8).

An excellent correlation is found between tensile strength σ_B and $\bar{M}_w$, while the $\epsilon_B/\bar{M}_w$ and $A/\bar{M}_w$ relations show some scatter, which however does not appear to be due to MWD effects.

Creep Measurement

The creep experiments were carried out in a circulating oven by applying a tensile weight to samples 6.3 mm. wide and 1.2 mm. thick. The elongation was determined as a function of time t by measuring the distance between two marks 40 mm. apart with a cathetometer. Two series of measurements were carried out, the first with high and the second with low tensile stresses. The first series was carried out at 23 ± 0.2°C. on all the samples, except polymers G and H (which broke immediately) with a tensile stress, based on the original cross-sectional area, of 1.25×10^7 dyne/cm.^{2} (about $^1/_{10}$ of the tensile strength σ_B). The creep curves were measured for 1.3×10^4 min., after which the load was removed and the recovery curves recorded for 6×10^4 min. Typical curves are shown in Figure 9.

In such tests the stress is not constant but increases continuously, since the cross-sectional area decreases. For purposes of comparison, the constant-load curves can be described by an equation of the form:[11]

$$\epsilon = kt^n \tag{2}$$

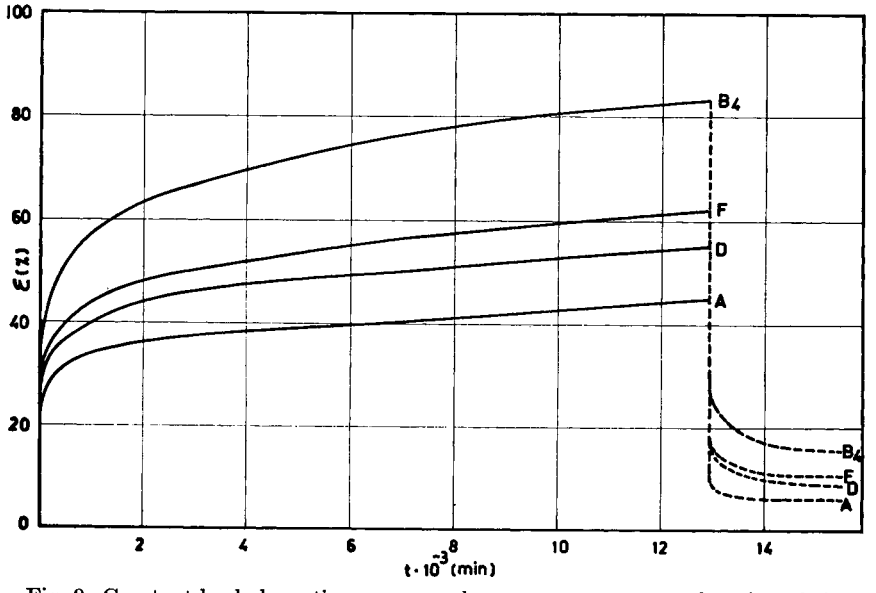

Fig. 9. Constant-load elongation curves and recovery curves, as a function of time, at 23°C. Initial tensile stress 1.25×10^7 dyne/cm.^{2}. Individual points not shown but indistinguishable from the curve.

TABLE IV
Creep Properties of the Plasticized Samples at 23°C.
at an Initial Tensile Stress of 1.25×10^7 dyne/cm.^{2}

Sample	Maximum elongation ϵ_m, %	Residual elongation ϵ_r, %	n
F1	45	2.5	0.078
F2	53	3.0	0.089
F3	58	3.0	0.099
F4	53	1.6	0.095
F5	50	3.0	0.094
F6	58	2.5	0.097
F7	50	1.6	0.098
F8	53	4.0	0.097
F9	48	2.5	0.097
F10	43	1.6	0.095
F11	54	3.3	0.099
A	45	2.5	0.089
B	50	2.5	0.090
C	50	2.5	0.089
D	55	5.0	0.097
E	58	5.0	0.103
F	62	5.5	0.110
B1	61	4.0	0.098
B2	52	4.0	0.099
B3	47	2.5	0.094
B4	83	8.0	0.120
B5	48	3.3	0.111
B6	50	3.3	0.112

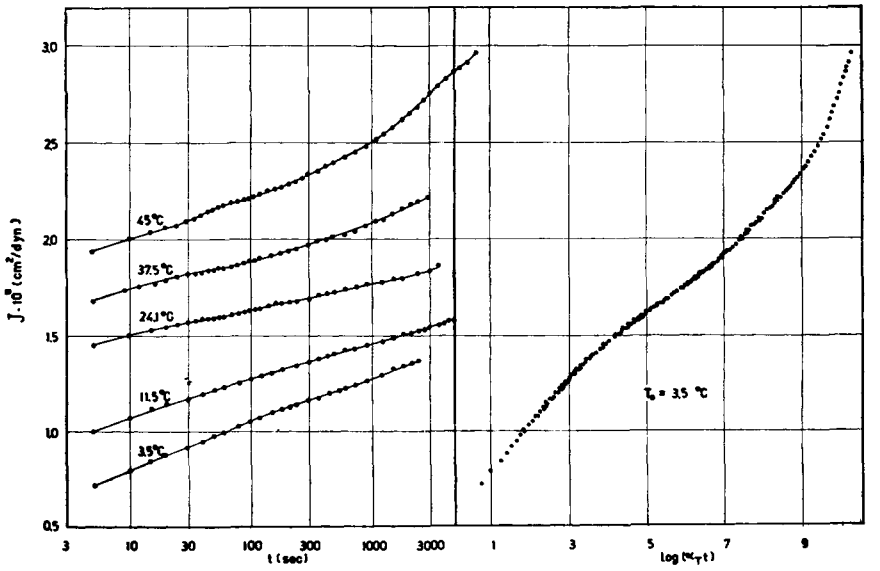

Fig. 10. Reduction to master curves of the creep data for fraction 1 by displacement of the curves along the log t scale. Tensile stress $\sigma = 3 \times 10^6$ dyne/cm.^{2}.

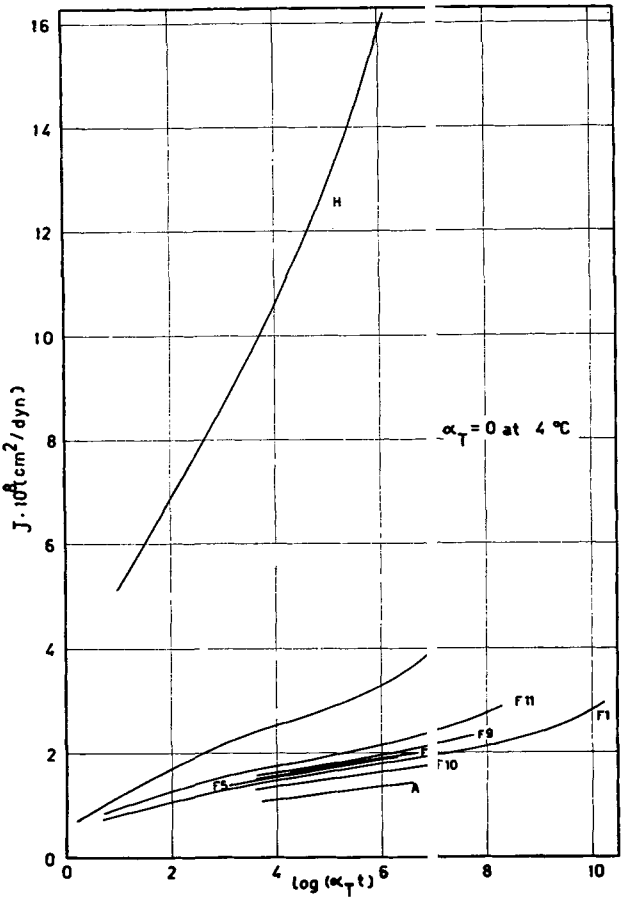

Fig. 11. J–log t curves for several samples, reduced to master curves at 4°C.

where n is an empirical parameter independent of the applied load. For $n = 1$ the straining process would be completely viscous in nature, while for $n = 0$ the strain would be independent of time as found for ideal rubbers.

The creep data have been found to follow eq. (2) very closely over the entire range of time, and from log–log plots of strain versus t the values of n have been obtained. They are collected in Table IV, together with the maximum elongation after 13,000 min. ϵ_m and the residual elongation after 60,000 min. of recovery ϵ_r. The values of n are around 0.1, which should indicate that the deformation process is mainly of elastic nature. The recovery curves show indeed that the irreversible elongation ϵ_r represents only a small fraction (less than 8%) of the maximum elongation ϵ_m.

Although the viscous contribution is so low, the viscoelastic process is far from being linear, and the recovery curves differ considerably from the creep curves. The rate of recovery is larger than the rate of creep at the beginning of the process, but it becomes smaller than the creep rate after

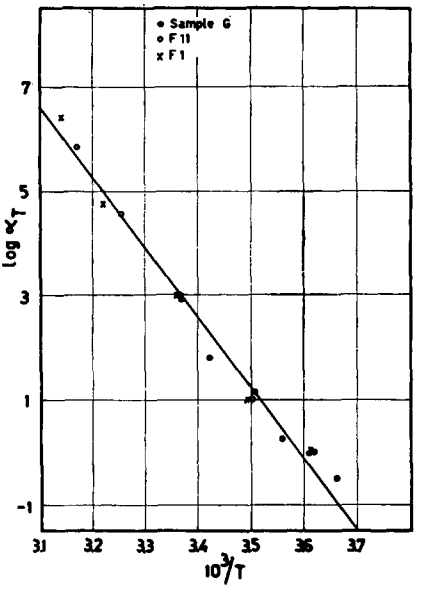

Fig. 12. Arrhenius plot of the shift parameters log a_T vs. $1/T$. The activation energy is 60 kcal./mole.

about 10^3 min. The recovery curves cannot be superimposed upon the creep curves.

It is difficult to find evidence of molecular weight effects on ϵ_m, ϵ_r, and n, although the molecular weight distribution seems to effect the time dependence of creep, as shown by the higher values of n found for the more disperse blends B4, B5, and B6.

The creep behavior at low stresses was investigated on several samples between 4 and 45°C. at tensile stresses from 10^6 to 3×10^6 dyne/cm.^{2}. Within this range, the viscoelastic behavior was found to be essentially linear, the compliance J being independent (at constant time) of the applied tensile load. Measurements were carried out for about 3000 sec., starting 3 sec. after loading the specimens. Plots of J versus log t were obtained, and they were easily reduced to a master curve by time–temperature superposition.[12] An example is shown in Figure 10 for fraction 1, while the J–log t curves for several samples, reduced to 4°C., are plotted in Figure 11. It can be seen that a molecular weight effect is evident only for fraction 11 and polymers G and H, whose $\bar{M}_w$ are very low, while the J–log t curves of all the other samples are situated in the same region. The amount by which the curves have been shifted along the log t axis, log a_T, when plotted versus reciprocal absolute temperature, gives an activation energy of about 60 kcal./mole, a value typical for relaxation processes taking place at temperatures not much above the glass transition temperature.[13] From Table II it is seen that T_g lies at about −40°C. for these samples.

DISCUSSION

According to the results of Table II, the melt flow behavior of plasticized PVC is strongly affected by the molecular weight and its distribution. The curves recorded during the mixing of the samples in the plastograph (Fig. 2) give an equilibrium torque T which tends to zero as $\bar{M}_w$ approaches zero, and increases rapidly with increasing $\bar{M}_w$ above 50,000 (Fig. 3). T can be considered a rough index of the viscosity of the melt at the temperature and shear conditions encountered in the mixing chamber. From a log–log plot of T versus $\bar{M}_w$, one can obtain the exponent of eq. (3):[12]

$$\eta = KM_w^{\alpha} \tag{3}$$

at the average shear rate of the rheometer. The value of α so obtained is about 1.7, which is half the "universal" value of 3.5, characteristic of the zero-shear rate of Newtonian viscosity of molten polymers. This can be attributed to the well-known decrease of α with increasing shear rate.[14,15] Two recent investigations have shown that T can be converted into more fundamental rheological data by means of appropriate calibrations of the rheometer.[16,17] According to Goodrich and Porter[16] and Blyler and Daane,[17] the average shear rate in the mixing chamber is about 50 sec.$^{-1}$ at 50 rpm, and the α value of 1.7 should therefore refer to these shear conditions. For the blends, T is lower than for fractions or polymers of equivalent $\bar{M}_w$ (Fig. 3), as found for the melt viscosity of other polymers in the non-Newtonian region.[18,19] Although these results have only a semiquantitative meaning because the melt temperature is not constant for all samples, it must be emphasized that the relations between T and $\bar{M}_w$ or $[\eta]$[9,10] hold only for samples having about the same MWD.

An overall analysis of the tensile and creep data shows that the recovery after long-term creep is almost complete, which means that the process is mainly due to retarded elastic deformation.

The properties measured at relatively low extensions (or stresses), namely Young's modulus E (Fig. 5) and creep results (Table IV and Fig. 11) are largely independent of molecular weight above $\bar{M}_w$ = 40,000, i.e., with the exception of polymers G and H. A slight influence of MWD is evident in the long-term creep, where the exponent n is sensibly increased by polydispersity.

The properties measured at high extensions, namely σ_B, ϵ_B, and A (Figs. 6–8) are strongly influenced by $\bar{M}_w$. From log–log plots, one can see that both σ_B and ϵ_B are roughly proportional to $\bar{M}_w^{1.3}$ and A to $\bar{M}_w^{2.7}$. No clear effects of MWD can be observed, provided the weight-average molecular weight is used as variable.

The recoverable character of the long-term creep of plasticized PVC can be taken as evidence that this polymer has a network structure. Several authors assume that in the network the macromolecules are bonded by small crystalline regions acting as crosslinks.[20–26] However, the absence of flow in the long-term creep above T_g is by no means restricted to PVC,

being present in such polymers as polystyrene,[27] butadiene–styrene copolymers,[28] and polydimethylsiloxane,[29] whose networks cannot be bonded by crystallites. Chain entanglements and association of chains through secondary bonds are probably acting as semipermanent crosslinks in these polymers. On the other hand, the presence of crystallites in plasticized PVC is confirmed by the temperature dependence of the viscoelastic properties[25,26] and by the results of x-ray diffraction studies.[30,31] Further evidence for the tendency of the PVC molecules to aggregate, even in dilute solutions, into compact clusters or crystallites is given by sedimentation[32] and light-scattering[33–35] results.

Also the stress–strain curves of the samples here investigated resemble those of rubbers, having the S-shaped form characteristic of a three-dimensional network, with a clear rise in the slope at elongations above 200% (Fig. 4). The upward curvature is, however, small, and the curves proceed almost linearly to their breaking points. The absence of a final steep ascent of the curves indicates[36] a small capacity of the network to crystallize and/or the absence of non-Gaussian effects before failure. For the equilibrium modulus of stable three-dimensional networks, the statistical theory of rubber elasticity predicts the equation

$$E = (3\rho RT/M_c)[1 - (2M_c/M_n)] \tag{4}$$

where ρ is the density, T the absolute temperature, M_c the molecular weight between crosslinks and $\bar{M}_n$ the number-average molecular weight before crosslinking.

Assuming that eq. (4) can be applied to the plasticized PVC samples here investigated, the constancy of the Young's modulus E above $\bar{M}_w$ = 40,000 (Fig. 5) and the absence of molecular weight effects on the creep results (Table IV) should be interpreted as evidence that the molecular weight between crosslinking M_c is constant and does not vary with the polymer molecular weight $\bar{M}_w$. Following eq. (4) the plateau value of E (7×10^7 dyne/cm.^{2}) would correspond to an M_c of about 1000. These results must be taken with care, because there could be an energy component added to the entropy component of the stress during deformation, while eq. (4) applies only to purely entropic processes.

Moreover, the nature and the topology of the PVC network are little known and they could differ considerably from those of rubbers.

For example, a substantial part of the molecules could not be bound to the network. The small E values of samples G and H could be explained on these grounds: according to eq. (4) both these samples should have roughly the plateau value of the modulus ($E = 7 \times 10^7$ dyne/cm.^{2}) because their molecular weight is several times larger than the value of M_c ($M_c = 10^3$) of the other samples. On the contrary, their moduli correspond to M_c of 2×10^3 and 6×10^3, respectively, which shows that their molecules are probably bonded to an imperfect network. For the same reason the blends containing samples G and H show a larger contribution of viscous flow to the creep process (Table IV).

The molecular weight dependence of the ultimate properties (Figs. 5–7) is not easily accounted for by simple models.

The tensile strength of rubbers, at constant degree of crosslinking, obeys an equation of the same form as eq. (4):[36]

$$\sigma_B = A - (B/\bar{M}_n) \tag{5}$$

which predicts an increase of σ_B with increasing $\bar{M}_n$, followed by a leveling off to an asymptotic value. Most of the tensile data on glassy or crystalline polymers are also plotted following eq. (5).[37] For the tensile strength of rubbers, Flory[36] interpreted this dependence on the basis that σ_B varies linearly with the proportion of the chains which is oriented by stretching and therefore crystallizes before failure.

Following Bueche[38] the tensile strength of rubbers should depend on $\bar{M}_n$ through a slightly different equation:

$$\sigma_B = A\,[1 - (2M_c/\bar{M}_n)]^{2/3} \tag{6}$$

which also predicts a leveling off of σ_B with increasing $\bar{M}_n$.

The tensile strength data of Table III cannot be described satisfactorily by eqs. (5) or (6), because the plots of σ_B and $\sigma_B^{3/2}$ versus $1/\bar{M}_n$ are scattered and not linear.

The plots of σ_B and $\sigma_B^{3/2}$ versus $1/\bar{M}_w$ are also curved, although less scattered. Both eqs. (5) and (6) fail therefore to describe the results of tensile testing.

One can interpret in a semiquantitative way the tensile strength results by assuming that the network crosslinks are not stable under stretching at high stresses.

The PVC structure would be therefore more similar to the dissociable network of gels than to the permanent network of rubbers. It is known that in associated systems the flow rate is determined by the breaking of bonds in the structure, and the strong dependence of σ_B on $\bar{M}_w$ could be due to the effect of $\bar{M}_w$ on the stability of the crystallite-bonded PVC network.

Unpublished data of this laboratory[39] seem to support this interpretation because they show that the melting point of PVC–cyclohexanone gels increases strongly with the polymer molecular weight.

References

1. G. Pezzin, G. Sanmartin, and F. Zilio-Grandi, *J. Appl. Polymer Sci.*, **11**, 1539 (1967).

2. R. N. Haward, B. Wright, G. R. Williamson, and G. Thackray, *J. Polymer Sci. A*, **2**, 2977 (1964).

3. G. Boccato, A. Rigo, G. Talamini, and F. Zilio-Grandi, *Makromol. Chem.*, **108**, 218 (1967).

4. G. Talamini and G. Vidotto, *Makromol. Chem.*, **100**, 48 (1967).

5. A. Nakajima, H. Hamada, and S. Hayashi, *Makromol. Chem.*, **95**, 40 (1966).

6. J. Bargon, K. H. Hellwege, and U. Johnsen, *Makromol. Chem.*, **95**, 187 (1966).

7. O. C. Böckman, *J. Polymer Sci. A*, **3**, 3399 (1965).

8. A. Guyot and J. P. Benevise, *Ind. Plast. Mod. (Paris)*, **13**, 37 (June 1961).

9. W. T. Blake, *Plastics Technol.*, **4**, 909 (1958).
10. P. Schmidt, *Kunststoffe*, **42**, 142 (1952).
11. R. Buchdahl and L. E. Nielsen, *J. Appl. Phys.*, **22**, 1344 (1951).
12. A. V. Tobolsky, *Properties and Structure of Polymers*, Wiley, New York, 1960.
13. L. E. Nielsen, *Mechanical Properties of Polymers*, Reinhold, New York, 1962, p. 14.
14. H. P. Schreiber, E. B. Bagley, and D. C. West, *Polymer*, **4**, 355 (1963).
15. R. A. Stratton, *J. Colloid Sci.*, **22**, 517 (1966).
16. J. E. Goodrich and R. S. Porter, *Polymer Eng. Sci.*, **7**, 45 (1967).
17. L. L. Blyler and J. H. Daane, paper presented at American Chemical Society Meeting, Division of Polymer Chemistry, Miami Beach, April 1967; *Polymer Preprints*, **8**, 433 (1967).
18. R. L. Ballman and R. H. M. Simon, *J. Polymer Sci. A*, **2**, 3557 (1964).
19. A. K. Van der Vegt, *Plastics Inst. Trans. (London)*, **32**, 165 (1964).
20. H. Leaderman, *Ind. Eng. Chem.*, **35**, 374 (1943).
21. W. Aiken, T. Alfrey, A. Janssen, and H. Mark, *J. Polymer Sci.*, **2**, 178 (1947).
22. F. P. Reding, E. R. Walter, and F. J. Welch, *J. Polymer Sci.*, **56**, 225 (1962).
23. A. T. Walter, *J. Polymer Sci.*, **13**, 207 (1954).
24. R. Sabia and F. R. Eirich, *J. Polymer Sci. A*, **1**, 2497, 2511 (1963).
25. R. B. Taylor and A. V. Tobolsky, *J. Appl. Polymer Sci.*, **8**, 1563 (1964).
26. M. C. Shen and A. V. Tobolsky, *Advan. Chem. Ser.*, **48**, 118 (1965).
27. L. E. Nielsen and R. Buchdahl, *J. Colloid Sci.*, **5**, 282 (1950).
28. M. A. Luftglass, W. R. Hendricks, G. Holden, and J. T. Bailey, *S.P.E. Tech. Papers*, **12**, paper XIV-6 (1966).
29. D. J. Plazek, W. Dannhauser, and J. D. Ferry, *J. Colloid Sci.*, **16**, 101 (1961).
30. T. Alfrey, N. Wiederhorn, R. Stein, and A. Tobolsky, *Ind. Eng. Chem.*, **41**, 701 (1949).
31. V. P. Lebedev, L. Y. Derlynkova, J. N. Razinskay, N. A. Okladnov, and B. P. Shtarkman, *Polymer Sci. USSR*, **7**, 366 (1965).
32. J. Hengstenberg and E. Schuch, *Makromol. Chem.*, **74**, 55 (1964).
33. G. Pezzin, G. Talamini, and N. Gligo, *Chim. Ind. (Milan)*, **46**, 648 (1964).
34. H. Janeschitz-Kriegl and A. J. Staverman, *Makromol. Chem.*, **44/46**, 241 (1961).
35. P. Kratochvil, *Collection Czechoslovak. Chem. Commun.*, **29**, 2767 (1964).
36. P. J. Flory, *Ind. Eng. Chem.*, **38**, 417 (1946).
37. O. Fuchs, in *Struktur und physikalisches Verhalten der Kunststoffe*, Vol. I, Nitsche and Wolf, Eds., Springer, Berlin, 1962.
38. F. Bueche, *Physical Properties of Polymers*, Interscience, New York, 1962.
39. G. Perzin and G. Talamini, unpublished results.

Received September 20, 1967